

See discussions, stats, and author profiles for this publication at: <https://www.researchgate.net/publication/228967910>

Motorcycle State Estimation for Lateral Dynamics

Article in *Vehicle System Dynamics* · November 2010

DOI: 10.1080/00423114.2012.656655

CITATIONS

39

READS

1,366

2 authors, including:



[Sven Jansen](#)

TNO

20 PUBLICATIONS 186 CITATIONS

[SEE PROFILE](#)

Some of the authors of this publication are also working on these related projects:



Effects of automation on road user behaviour and performance [View project](#)



(CCAM Platform) Support for the implementation of the single platform for open road testing and pre-deployment of cooperative, connected, automated and autonomous mobility [View project](#)

Motorcycle State Estimation for Lateral Dynamics

A.P. Teerhuis*, S.T.H. Jansen*

* TNO Automotive

Steenovenweg 1, 5708 HN Helmond, The Netherlands

e-mail: arjan.teerhuis@tno.nl

Keywords: Extended Kalman Filter, Motorcycle Model

Abstract

The motorcycle lean (or roll) angle development is one of the main characteristics of motorcycle lateral dynamics. Control of motorcycle motions requires an accurate assessment of this quantity and for safety applications also the risk of sliding needs to be considered. Direct measurement of the roll angle and tyre slip is not available; therefore a method of model-based estimation is developed to estimate the state of a motorcycle. This paper investigates the feasibility of such a Motorcycle State Estimator (MCSE). A simplified analytic dynamic model of a motorcycle is developed by comparison to an extended multi-body model of the motorcycle, designed in Matlab/SimMechanics. The analytic model is used inside an Extended Kalman Filter (EKF). Experimental results of an instrumented Yamaha FJR1300 motorcycle show that the MCSE is a feasible concept for obtaining signals related to the lateral dynamics of the motorcycle.

1 Introduction

Automotive safety applications become more and more common in today's vehicles, trucks and also motorcycles. Vehicle stabilization systems such Anti-lock Brake Systems (ABS) and Electronic Stability Control (ESC) are introduced since the late 1970s and have now become almost standard in every passenger car. Safety applications, such as airbags, collision mitigation/avoidance systems, adaptive cruise control, lane departure warnings, etc., have become available on the market more recently. All these systems are mainly applied to two-track vehicles, i.e. which have at least four wheels. For single-track (two-wheeled) vehicles such as motorcycles, both the market for these system seems more conservative and additionally the applications can be more complex compared to two-tracked vehicles due to the system dynamics, limited space, etc. Despite of this, safety applications gradually are finding their way to the motorcycle market as well. Two examples of such systems are ABS and airbags (either on the motorcycle itself or in the jacket). To effectively deploy such systems, one has to know reliably what the current state of the motorcycle is. For these applications, several sensors can be used (e.g. lateral acceleration, yaw rate, wheel speeds), which are known from the two-tracked vehicle applications. One of the important differences however concerns the roll angle. For two-track vehicles, the roll angle normally is very small, in contrary to motorcycles. Roll angles exceeding 40° are no exception. For safety systems that intervene in the driveline and/or in the braking system it is eminent to consider the roll angle and avoid interventions at large roll angles as they may destabilize the motorcycle. In this paper, we will describe the development of an Extended Kalman Filter (EKF) to determine the roll angle using low-cost sensors, resulting in the Motorcycle State Estimator (MCSE). The MCSE algorithm is written in C-code and compiled onto a real-time platform, dSPACE MicroAutobox, which is located in the top case of the experimental motorcycle. A description of the motorcycle and its instrumentation is given in section 2.

2 Experimental motorcycle

In this research a Yamaha FJR1300 motorcycle is used which is equipped with several sensor systems (see Fig.1)). In addition to the sensors that are used for the motorcycle state estimator (MCSE) it is equipped with sensors that provide a reference for the output of the MCSE and additional signals that have been used to validate the simulation models that are described in the next sections.



Figure 1. The experimental motorcycle: a Yamaha FJR1300.

Below a short overview of each of the systems on the FJR1300 motorcycle is presented (the numbers below correspond to the numbers in Figure 1):

1. **Steering angle encoder and steering torque:** the signal from the encoder is used as input to the MCSE (δ), while the steering torque is used for model development only.
2. **6-DOF motion sensor unit:** this system measures 3 accelerations and 3 rotational velocities. For use in the MCSE, only roll rate ($\dot{\phi}$), yaw rate ($\dot{\psi}$) longitudinal acceleration (a_x) and lateral acceleration (a_y) are used as so-called sensor inputs to the estimator.
3. **reference measurement system** [3]: this system measures 3 accelerations, 3 rotational velocities and combines them with GPS positioning to determine (a.o.) roll angle, pitch angle, forward and lateral velocity. The data from this system is used to evaluate the MCSE, and for validation of the simulation models.
4. **GPS antenna:** this system is used by the *reference measurement system*.
5. **Front wheel speed sensor:** this sensor is standard on an Yamaha FJR1300, where it is used for the ABS system. The wheel speed is used as an input to the state estimator (ω_f)
6. **Rear wheel speed sensor:** The wheel speed is used as an input to the state estimator (ω_r)
7. **dSPACE MicroAutobox** [4]: This is an ECU intended for Rapid Control Prototyping. It is used in this application to collect all sensor information and to run the estimator in real time.

8. **Laptop:** the laptop is connected to the MicroAutobox and it is used to monitor the output of the state estimator.
9. **Wi-Fi antenna:** When the motorcycle is moving, the laptop inside the top case can not be operated. Therefore another PC (which is based at a fixed location near the test-track or inside a moving car) is connected through a Wi-Fi network to the laptop. A so-called remote desktop connection enables the control over the laptop that is located inside the top case.

3 Multi-body model of the experimental motorcycle

The model that is used in the MCSE is a minimal complexity representation of the actual motorcycle in order to minimize the set of analytical equations and related CPU requirements. Several of the dynamics that are present on a real motorcycle are not considered in the internal MCSE model. To substantiate these simplifications, a multi-body model of the Yamaha FJR1300 has been developed to investigate the effects of neglecting parts of the dynamics. Additionally the Multi-Body model has been used for evaluation of the MCSE output that can not be measured (e.g. tyre forces and slip angle). The model is made in Matlab/SimMechanics, and it has been validated with measurements on the experimental motorcycle. For setting up the model, the motorcycle has been disassembled into several parts of which the dimensions and inertia is measured. The results have been used to setup the rigid bodies in the multi-body model, see Figure 2.



Figure 2. The multi-body model of the experimental motorcycle consists of 6 rigid bodies and a rigid driver

The following rigid bodies are used in the SimMechanics model:

1. Rear wheel
2. Rear suspension arm (swing arm)

3. Motorcycle main frame
4. Sprung part of the front fork (including the handle bars)
5. Unsprung part of the front fork
6. Front wheel
7. Rider (considered to be rigid and fixed with respect to the motorcycle main frame)

The inertia of the rider has been calculated by feeding his biometric data and posture into the MADYMO program for human body modelling [REF?]. The remaining body masses and inertias have been determined experimentally. The characteristics of the front and rear suspension elements were measured separately on a test-rig. The tyre characteristics have been modelled using TNO's Magic Formula software, of which the parameters were determined from tyre experiments with the measurement truck from TNO Automotive [5].

To validate the performance of the multi-body model, the *Virtual Motorcycle* (VMC), the actual measurements of the experimental motorcycle have been replayed with the VMC. To track the forward velocity, a PID controller is used to drive the rear wheel and brake the front wheel. The measured steering torque of the experimental motorcycle is applied directly as a feedforward to the steering system of the VMC, while at the same time, a PID feedback controller adds small corrections to the feedforward steering torque in order to track the measured roll angle. An example of the model performance for steady state cornering and slalom manoeuvres can be seen in respectively Figure 3 and Figure 4. As can be seen the relation between steering input and roll response of the motorcycle is matched well for both manoeuvre types. Note that the applied steering torque to the VMC differs not much from the one measured on the real motorcycle. This implies that the steering torque feedback controller has no need to modify the feedforward steering torque. From this it can be concluded that the VMC is a good representation of the actual motorcycle.

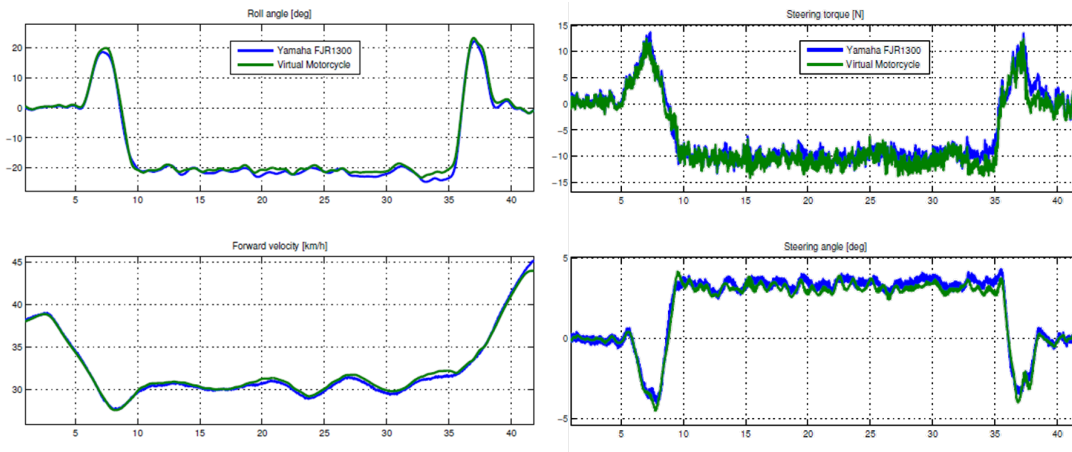


Figure 3. Comparison between *Virtual Motorcycle* (green) and the experimental results (blue) for a steady state circle manoeuvre. Roll angle (top left), forward velocity (bottom left), steering torque (top right) and steering angle (bottom right)

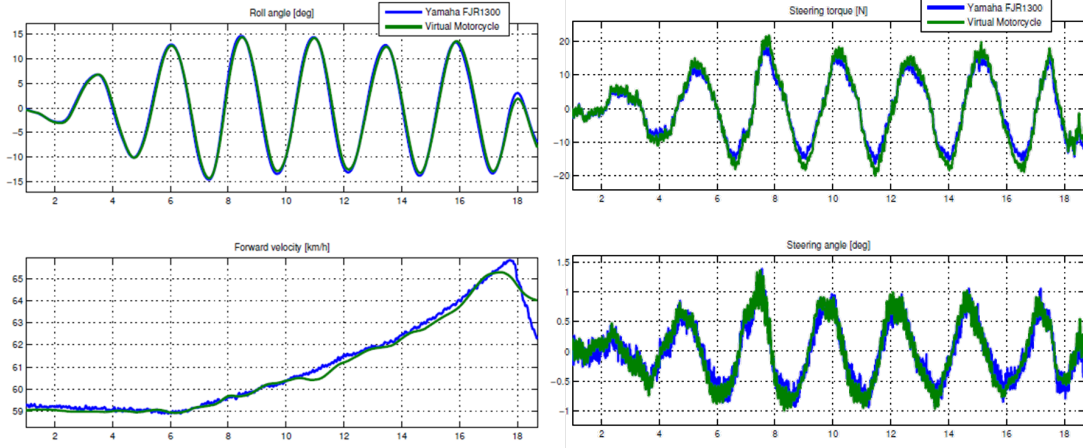


Figure 4. Comparison between *Virtual Motorcycle* (green) and the experimental results (blue) for a slalom manoeuvre. Roll angle (top left), forward velocity (bottom left), steering torque (top right) and steering angle (bottom right)

4 Motorcycle model for use inside the State Estimator

The developed State Estimator is a so-called Extended Kalman Filter, which is a model-based algorithm that uses an internal representation of the motorcycle. Obviously, the first step in designing such an estimator is to develop a suitable model that captures the behaviour of interest with sufficient accuracy (in this case roll response), but on the other hand it should be simple, to avoid large calculation times. The multi-body motorcycle model described in the previous section has been used to verify which degrees of freedom can be removed from that model without compromising the accuracy for describing the roll response of the motorcycle. From this effort it was concluded that at least the following degrees of freedom (DOFs) should be part of the internal estimator model:

- **Forward translation:** (quasi) position X , velocity v_x and its derivative \dot{v}_x .
- **Lateral translation:** (quasi) position Y , velocity v_y and its derivative \dot{v}_y .
- **Yaw angle:** angle Ψ , rate r and acceleration \dot{r} .
- **Motorcycle roll:** angle φ , rate $\dot{\varphi}$ and acceleration $\ddot{\varphi}$.
- **Steering angle:** angle δ , rate $\dot{\delta}$ and acceleration $\ddot{\delta}$.
- **Front wheel rotations:** angle W_f , rate ω_f and acceleration $\dot{\omega}_f$.
- **Rear wheel rotations:** angle W_r , rate ω_r and acceleration $\dot{\omega}_r$.

Basically, the motorcycle is modelled as a rigid frame with the rear wheel attached and a rigid front fork with the front wheel; no suspension is considered. Compared to the setup as proposed by Pacejka [1], the applied model in the MCSE is not restricted to small roll angles but it does not consider chassis flexibility.

The internal model is schematically presented in Figure 5. The next sections describe the steps to derive the equations of motion, and to reduce the set of equations..

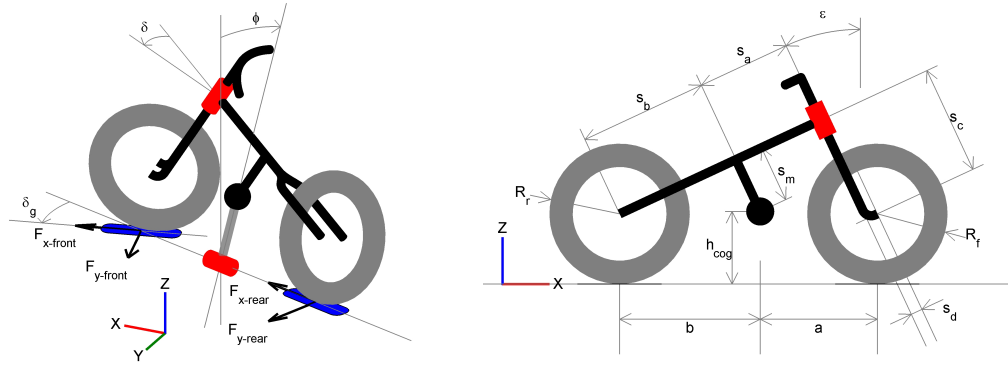


Figure 5. Schematic representation of the motorcycle model that is used in the Extended Kalman Filter.

4.1 Motorcycle kinematics

First, the kinematics of the motorcycle model are determined. The kinematic model is set up using $[4 \times 4]$ coordinate transformation matrices [REF], of the form:

$$T = \left(\begin{array}{ccc|c} \cdot & \cdot & \cdot & \cdot \\ \cdot & \mathbf{R} & \cdot & \underline{p} \\ \cdot & \cdot & \cdot & \cdot \\ 0 & 0 & 0 & 1 \end{array} \right) \quad (1)$$

Where \mathbf{R} is a $[3 \times 3]$ rotation matrix and \underline{p} is a $[3 \times 1]$ translation vector:

$$\mathbf{R} = \begin{pmatrix} R_{xx} & R_{xy} & R_{xz} \\ R_{yx} & R_{yy} & R_{yz} \\ R_{zx} & R_{zy} & R_{zz} \end{pmatrix}; \underline{p} = \begin{pmatrix} p_x \\ p_y \\ p_z \end{pmatrix} \quad (2)$$

The complete kinematics of the motorcycle is built up from multiple of such transformation matrices, and it is a combination of translations and rotations in a well defined order.

Let Θ be a transformation function for either translation or rotation of a coordinate system. For translation along one of the three orthonormal axes directions, the function is defined as: Θ_i^{trans} , where $i = x, y, z$. Rotation around one of the three axes is defined as: Θ_i^{rot} , where $i = x, y, z$. This implies that there are six transformation functions, three for a translation over a distance a

and three for a rotation angle β :

$$\begin{aligned}
\Theta_x^{trans}(a) &= \left(\begin{array}{ccc|c} 1 & 0 & 0 & a \\ 0 & 1 & 0 & 0 \\ 0 & 0 & 1 & 0 \\ \hline 0 & 0 & 0 & 1 \end{array} \right), & \Theta_x^{rot}(\beta) &= \left(\begin{array}{ccc|c} 1 & 0 & 0 & 0 \\ 0 & \cos(\beta) & -\sin(\beta) & 0 \\ 0 & \sin(\beta) & \cos(\beta) & 0 \\ \hline 0 & 0 & 0 & 1 \end{array} \right) \\
\Theta_y^{trans}(a) &= \left(\begin{array}{ccc|c} 1 & 0 & 0 & 0 \\ 0 & 1 & 0 & a \\ 0 & 0 & 1 & 0 \\ \hline 0 & 0 & 0 & 1 \end{array} \right), & \Theta_y^{rot}(\beta) &= \left(\begin{array}{ccc|c} \cos(\beta) & 0 & \sin(\beta) & 0 \\ 0 & 1 & 0 & 0 \\ -\sin(\beta) & 0 & \cos(\beta) & 0 \\ \hline 0 & 0 & 0 & 1 \end{array} \right) \\
\Theta_z^{trans}(a) &= \left(\begin{array}{ccc|c} 1 & 0 & 0 & 0 \\ 0 & 1 & 0 & 0 \\ 0 & 0 & 1 & a \\ \hline 0 & 0 & 0 & 1 \end{array} \right), & \Theta_z^{rot}(\beta) &= \left(\begin{array}{ccc|c} \cos(\beta) & -\sin(\beta) & 0 & 0 \\ \sin(\beta) & \cos(\beta) & 0 & 0 \\ 0 & 0 & 1 & 0 \\ \hline 0 & 0 & 0 & 1 \end{array} \right) \quad (3)
\end{aligned}$$

The transformation functions Θ can be multiplied to obtain a total transformation matrix from one origin to the other. This is explained in Figure 6. For example, take the moving origin of the motorcycle (O). Starting at the global reference frame (G), we first translate in the forward (X) direction, then in lateral (Y) direction and finally rotation along the vertical axis (Ψ):

$${}^O T_M = \Theta_x^{trans}(X) \cdot \Theta_y^{trans}(Y) \cdot \Theta_z^{rot}(\Psi) \quad (4)$$

Any point in the O -frame can be expressed in coordinates of G by multiplying the transformation matrix ${}^G T_O$ with the position vector of the O -based point (${}^O \underline{p}$):

$${}^G \underline{p} = {}^G T_O \cdot {}^O \underline{p} \quad (5)$$

The moving origin O of the motorcycle is chosen to be exactly below the overall centre of gravity, with respect to the global axis frame G . The front and rear wheel axis frames A and B are determined with respect to the moving origin O , as is the main frame centre of gravity F . The other origins X and Y are set up with respect to the main frame's centre of gravity F . The location and definition of each origin is schematically presented in Fig. 6.

$$\begin{aligned}
{}^O T_M &= \Theta_x^{trans}(X) \Theta_y^{trans}(Y) \Theta_z^{rot}(\Psi) \\
{}^M T_A &= \Theta_x^{trans}(a) \Theta_z^{rot}(\delta_g) \\
{}^M T_B &= \Theta_x^{trans}(-b) \\
{}^M T_F &= \Theta_x^{rot}(\varphi) \Theta_z^{trans}(h_{cog}) \\
{}^F T_X &= \Theta_y^{rot}(\epsilon) \Theta_z^{trans}(-s_m) \Theta_x^{trans}(s_a) \Theta_z^{rot}(\delta) \Theta_z^{trans}(-s_c) \Theta_x^{trans}(s_d) \Theta_y^{rot}(W_f) \\
{}^F T_Y &= \Theta_y^{rot}(\epsilon) \Theta_z^{trans}(-s_m) \Theta_x^{trans}(-s_b) \Theta_y^{rot}(W_r) \quad (6)
\end{aligned}$$

For small steering angles we may substitute the ground steering angle (δ_g) similar to [1]:

$$\delta_g = f(\varphi, \delta) = \delta \frac{\cos \epsilon}{\cos \varphi} \quad (7)$$

Now that all positions and orientations of each point of interest is known, we can use partial differentiation techniques, for both the time t as well as the generalized coordinates q , to obtain the (angular) velocities, \dot{q} , and the (angular) accelerations, \ddot{q} .

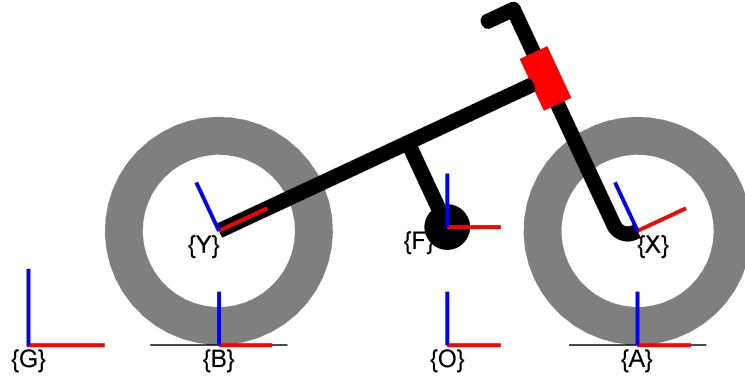


Figure 6. Location of all body-oriented axis frame origins (red and blue lines represent the x and z axis respectively).

4.2 Motorcycle dynamics

At this point, the motorcycle kinematics equations are known. This information is essential for deriving the dynamic equations of the motorcycle. Here we will use the modified Lagrange method to solve the equations of motion, similar as explained in [1]. In general, the set of Lagrange equations is of the following form in which q represents the degrees of freedom as listed above:

$$\frac{d}{dt} \frac{\partial T}{\partial \dot{q}_i} - \frac{\partial T}{\partial q_i} + \frac{\partial V}{\partial q_i} = Q_i \quad (8)$$

Where:

- $T = T(\dot{q}, q)$: Kinetic energy
- $V = V(\dot{q}, q)$: Potential energy
- $Q = Q(\dot{q}, q, \underline{u}^*)$: Generalized external forces

And:

$$\begin{aligned} \underline{q} &= [X \ Y \ \Psi \ \varphi \ \delta \ W_f \ W_r]^T \\ \underline{\dot{q}} &= [\dot{v}_x \ \dot{v}_y \ \dot{r} \ \dot{\varphi} \ \dot{\delta} \ \dot{\omega}_f \ \dot{\omega}_r]^T \\ \underline{\ddot{q}} &= [\ddot{v}_x \ \ddot{v}_y \ \ddot{r} \ \ddot{\varphi} \ \ddot{\delta} \ \ddot{\omega}_f \ \ddot{\omega}_r]^T \\ \underline{u}^* &= [F_x^f \ F_x^r \ F_y^f \ F_y^r \ M_x^f \ M_x^r \ M_{steer} \ M_{drive} \ M_{brake}^f \ M_{brake}^r]^T \end{aligned} \quad (9)$$

Note that the input vector \underline{u}^* considers the acting forces and moments (i.e. tyre forces F_x , F_y and moments M_x , steer torque M_{steer} , drive torque M_{drive} and brake torques M_{brake}) on the system, however in section 4.3, this input vector will be modified to the sensor signals designated for the MCSE.

The set of Lagrange equations of Eq. 8 can be solved for the second derivative of generalized coordinate vector $\underline{\ddot{q}}$:

$$\underline{\ddot{q}} = L(\dot{q}, q, \underline{u}^*) \quad (10)$$

As mentioned before, we have used the modified Lagrange method to set up the equations of motion, which makes use of so-called *quasi-coordinates*, being the positions, X and Y , and the orientations Ψ , W_f and W_r . These quasi-coordinates are used to set up and solve Eq.8, but have no use in describing the roll response and overall dynamics of the motorcycle. Therefore, these five quasi-coordinates are removed from the generalized coordinates vector q (but not its derivatives \dot{q} and \ddot{q}). In Eq.10 the quasi-coordinates will be substituted with zeros.

Now, the equations of motion are known, however, they have to be converted into the general state-space form for non-linear systems:

$$\begin{aligned}\dot{\underline{x}}^* &= f(\underline{x}^*, \underline{u}^*) \\ \underline{z} &= h(\underline{x}^*, \underline{u}^*)\end{aligned}\tag{11}$$

Where x^* is the state-vector, u^* the input vector and z the vector containing the system outputs (sensor vector). The state vector x^* is constructed using the generalized coordinates vector:

$$\underline{x} = [\dot{q} \quad q^*]^T = [v_x \quad v_y \quad r \quad \dot{\varphi} \quad \dot{\delta} \quad \omega_f \quad \omega_r \quad \varphi \quad \delta]^T\tag{12}$$

Where q^* contains all but the quasi-coordinates from q .

4.3 Tyre model

So far, the tyre forces and moments have been defined as external input through the input vector u^* in Eqn. 9. However, there are no measurements available for the individual tyre forces and moments, so they are removed from the input vector. Instead they are considered by substituting the tyre force input equations by a tyre model as part of the dynamics equations. In this feasibility study a linear tyre model is used that considers slip angles and inclination angles. The model considers longitudinal force F_x , lateral forces F_y and overturning moment M_x . The aligning moment is neglected:

$$\begin{aligned}F_x^f &= F_x^f(\kappa_f, \gamma_f) &= C_1 \cdot \kappa_f + C_2 \cdot \gamma_f \\ F_x^r &= F_x^r(\kappa_r, \gamma_r) &= C_3 \cdot \kappa_r + C_4 \cdot \gamma_r \\ F_y^f &= F_y^f(\alpha_f, \gamma_f) &= C_5 \cdot \alpha_f + C_6 \cdot \gamma_f \\ F_y^r &= F_y^r(\alpha_r, \gamma_r) &= C_7 \cdot \alpha_r + C_8 \cdot \gamma_r \\ M_x^f &= M_x^f(\gamma_f) &= C_9 \cdot \gamma_f \\ M_x^r &= M_x^r(\gamma_r) &= C_{10} \cdot \gamma_r\end{aligned}\tag{13}$$

As can be seen in Eq. 13, the equations do not depend on the vertical tyre forces nor on the longitudinal slip. This implies that the MCSE, may not be accurate for either large longitudinal accelerations (or decelerations) due to the load changes on the tyres and significant longitudinal slip. Generally the lateral slip angles remain small for a motorcycle tyre, however at large(r) roll angles the linear assumption for inclination may not be valid for lateral tyre forces.

4.4 State- and input vector rearrangement

Due to the substitution of the tyre model equations in the Lagrange equations from Eq. 10, the input vector reduces to steer torque, brake torques and drive torque, however driver inputs to the system other than steering command cannot be measured on the instrumented FJR1300 motorcycle.

The remaining moments are driver inputs to the system that cannot be measured at all, their results (i.e. steering angle and wheel speeds) however can be measured. Therefore we will remove the dynamics from the system equation $f(\underline{x}^*, \underline{u}^*)$ and move the steering angle and wheel speed variables from the state vector to the input vector.

The target for the MCSE is to operate with a minimal set of sensors. It is chosen to use steering angle and wheel speeds as inputs, instead of steering torque and drive/brake torques. As a result the steer dynamics and wheel dynamics are removed from the system equation $f(\underline{x}^*, \underline{u}^*)$, and the steering angle δ and wheel speeds ω_f and ω_r respectively are transferred to the input vector. The state vector x is reduced to longitudinal velocity v_x , lateral velocity v_y , yaw rate r , roll rate $\dot{\varphi}$, and roll angle φ . The sensor vector z contains longitudinal acceleration a_x , lateral acceleration a_y , yaw rate $\dot{\psi}$ and roll rate $\dot{\varphi}$. Note that the longitudinal acceleration signal is included for enhancement of the forward speed estimation.

The resulting system now becomes:

$$\begin{aligned}\dot{\underline{x}} &= f(\underline{x}, \underline{u}) \\ \underline{z} &= h(\underline{x}, \underline{u})\end{aligned}\tag{14}$$

where:

$$\begin{aligned}\underline{u} &= [\delta \quad \omega_f \quad \omega_r]^T \\ \underline{x} &= [v_x \quad v_y \quad r \quad \dot{\varphi} \quad \varphi]^T \\ \underline{z} &= [a_x^s \quad a_y^s \quad \dot{\psi}^s \quad \dot{\varphi}^s]^T\end{aligned}\tag{15}$$

5 Motorcycle State Estimator

In this section the design of the Motorcycle State Estimator is discussed.

5.1 Extended Kalman Filter

The model equations from Eqn. 15 are nonlinear, mainly due the roll angle which can take on values well beyond the linear assumptions. A so-called Extended Kalman Filter (EKF) has been used [2] for the state estimator, as this method is suited for non-linear systems. TNO has adapted this method earlier in it's Vehicle State Estimator (VSE) for passenger cars in order to account for non-linear tyre behaviour and as a result, the VSE gives reliable lateral slip estimation over the full operating range [6, 7]. In principle, an EKF is an algorithm that minimizes the deviation between measured and estimated system response (measurement error $e_z = z - h(x)$) by adjusting the state vector x of the internal model. Deviations may exist due to limitations of the internal model and from disturbances on measurement signals. The EKF method assumes that the deviations can be represented as Gaussian distributed noise N (w for model deviations, v for measurement deviations), characterised by matrices Q and R respectively:

$$\begin{aligned}\dot{\underline{x}} &= f(\underline{x}, \underline{u}, \underline{w}) \\ \underline{y} &= h(\underline{x}, \underline{u}, \underline{v}) \\ \underline{w} &\sim N(0, Q) \\ \underline{v} &\sim N(0, R)\end{aligned}\tag{16}$$

A full explanation of the Extended Kalman Filter can be found in [2].

5.2 Practical application

Using the EKF on the motorcycle requires several steps. First the parameters of the internal model need to be optimized to obtain a close match with the motorcycle roll angle response to steering input. The model dynamics response has been confirmed using equations 8 and 9, i.e. using the description prior to model reduction. The general response to steering input is governed by the tyre force and moment generation, and an optimization was made for the tyre model parameters using the reduced model equations 14 and 15. For both steps the use of the VMC multi-body model was required.

Secondly, the so-called noise matrices Q and R in Eqn. 16 need to be defined. The matrix Q concerns model accuracy, and its contents reflect the accuracy of the model states compared to the real system. The values of matrix Q may be different for different motorcycle types. The matrix R relates to the accuracy of the sensors used on the motorcycle and the sensor model equations. Determining the contents of both noise matrices which are robust for a large variety of manoeuvres has been the most time consuming task during the development of the MCSE.

6 Experimental results

To test the performance of the MCSE on a real motorcycle, the EKF algorithm has been applied on a dSPACE MicroAutoBox (item 7 in Figure 1), which is a real-time control prototyping platform. The MCSE algorithm runs at a sample rate of 100 Hz. A number of different manoeuvres has been performed, ranging from steady-state cornering to extreme handling courses. During all manoeuvres, the MCSE algorithm delivered satisfactory results. Some examples are discussed below.

6.1 Steady state circle with increasing forward velocity

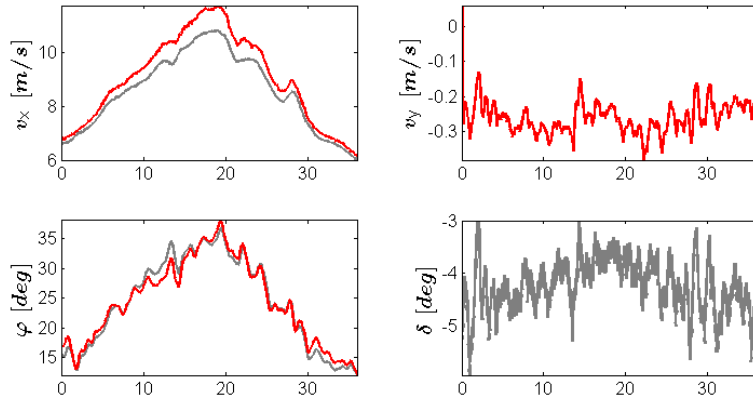


Figure 7. State estimator results of a fixed radius circle test with increasing velocity. Grey signals are reference measurements, red signals are estimated.

Figure 7 shows the result of a driving test with fixed radius and a gradual change of velocity. As can be seen there is a close match of the estimated and measured roll angle of the motorcycle. The velocity however shows a deviation which is related to roll angle of the motorcycle. Two of the

inputs to the estimator algorithm are the wheel speed velocities (see Eqn. 15). These are used to determine the longitudinal tyre slip κ_f and κ_r of the front and rear wheel respectively, using the estimated forward velocity v_y of the state vector x . For increasing roll angles, the tyre effective rolling radius reduces, which leads to too large values of κ . The roll angle effect on effective rolling radius is not (yet) accounted for in the MCSE, and as a result the estimated forward speed is too high during cornering motions.

6.2 Slalom manoeuvre

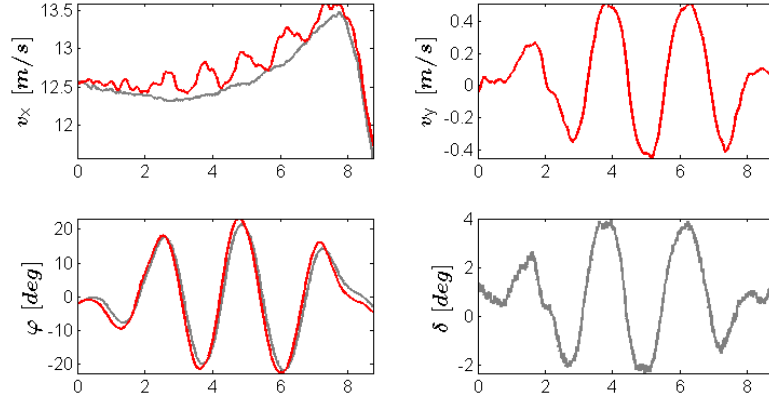


Figure 8. State estimator results of a slalom at constant forward velocity. Grey signals are reference measurements, red signals are estimated.

The results of a slalom manoeuvre are presented in Figure 8. The object for this test was to maintain a constant velocity. Due to roll angle effects on effective rolling radius (as discussed in the previous section) a variation on the velocity related to the roll angle of the motorcycle is also observed for this experiment. The roll angle is matched quite well also for this slalom test.

6.3 Handling track

Despite not being designed for large forward velocity changes, the MCSE is also evaluated for a handling track manoeuvre, see Figure 9. From the figure it can be seen that a large variation of velocity occurs during this test, and also a large range of roll angles occurs. The deviations between the measured and estimated forward velocity are due to the roll angles as explained above. The match in roll angle is reasonably well, except for very large roll angles. Note that the tyre characteristics in the MCSE are assumed linear, and this and other simplifications in tyre behaviour (e.g. constant load) are causing the deviations. Moreover, the driver behaviour (lean position) also affects the results. Still however the MCSE seems to be quite robust for all these effects.

7 Conclusions

An Extended Kalman Filter has proven to be a feasible way for creating a Motorcycle State Estimator for lateral motions with sufficient accuracy and practical computation demands.

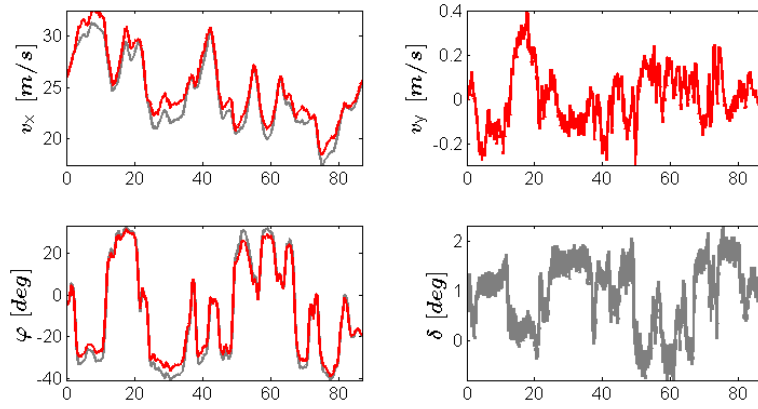


Figure 9. State estimator results of a run on the handling track. Grey signals are reference measurements, red signals are estimated.

The MCSE concept has been evaluated for roll angles up to 40 degrees, and basically the performance can be related to some important simplifications in the internal model of the MCSE. The internal model description neglects chassis flexibility and suspension effects and considers small steer angles only. The benefits of adding chassis flexibility is not easily predicted, but it is expected that inclusion of suspension effects and related degrees of freedom (i.e. pitch and heave) will improve the accuracy of the MCSE under braking and accelerating conditions.

The tyres are modelled as a rigid disc with a simple linear description of the contact slip forces. Inclusion of a tyre cross section description in the internal tyre model will improve the accuracy of estimation for vehicle speed, as that extension considers the increase in wheel speed due for larger roll angles. Modelling the non-linearities in tyre slip behaviour will improve the accuracy under large(r) roll angles and corresponding lateral accelerations.

8 Future work

With this research, the basis has been presented for a feasible motorcycle state estimator, which can be used in motorcycle control systems. To improve the performance for a wider application range, future development is aimed to extend the internal model description for better accuracy. The above mentioned suspension effects and extension of the tyre model will be investigated. The number of required sensors however should be minimized. More test drives have to be performed to check the robustness of the algorithm under several different (un-modelled) situations.

9 Acknowledgement

The authors would like to thank Mr. Shigeru Fujii and Mr. Souichi Shiozawa from Yamaha Motor Corporation for their support. Additionally Bart van Daal is thanked for his contributions in experimental work during his graduation project at TNO.

REFERENCES

- [1] H. B. Pacejka, *Tyre and Vehicle Dynamics*, Butterworth and Heinemann, Oxford, 2002.
- [2] Dan Simon, *Optimal State Estimation*, John Wiley & Sons, Hoboken, 2006.
- [3] <http://www.oxts.com/RT3100>
- [4] <http://www.dspace.com>
- [5] <http://www.delft-tyre.nl>
- [6] J. Zuurbier, P. Bremmer, *State Estimation for Integrated Vehicle Dynamics Control*, Proceedings AVEC '02 (#094), Hiroshima (Japan), 2002.
- [7] J. Zuurbier, N.J. Schouten, R. Leenen, *Central State Estimator for Vehicle Control Systems*, Proceedings, JSAE (paper number 20075048), May 2007.